Angewandte International Edition Chemie

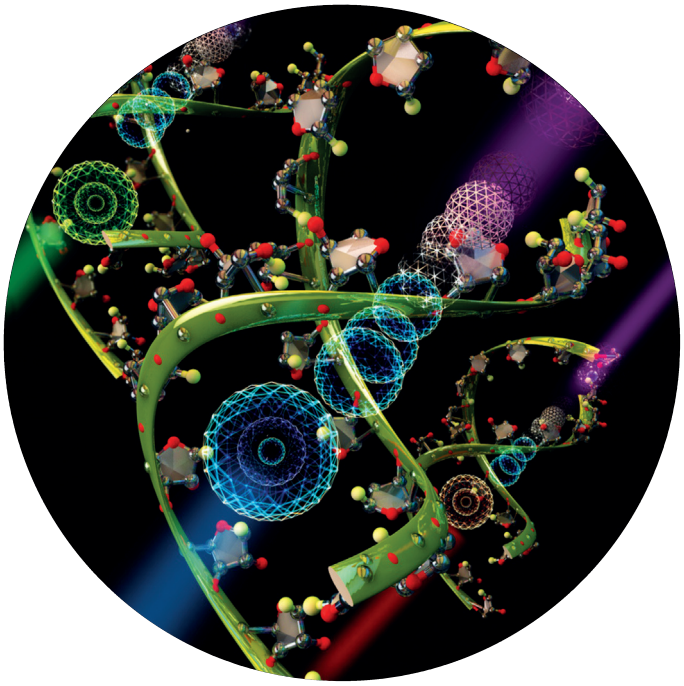

... of short-sequence microRNAs is very challenging. In their Communication on page 10024 ff. N. Hildebrandt and co-workers present a single-step "mix-and-measure" FRET assay for the multiplexed detection of different microRNAs. The careful design of the biophotonic probe and time-gated FRET from a luminescent Tb complex to three difference fluorescent dyes are crucial to this microRNA test for multiplexed clinical diagnostics.

Cluster Compounds

The atomicity of subnanometer platinum clusters significantly influences their catalytic activity. In their Communication on page 9810 ff., K. Yamamoto et al. report Pt_{19} as the most catalytically active species for oxygen reduction.

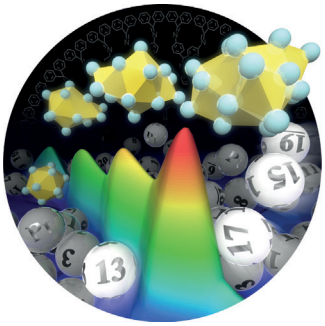

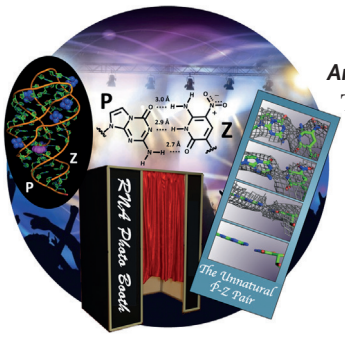

Artificial Nucleotides

The first functional RNA molecule containing the artificial nucleotides Z and P is prepared and structurally characterized by Piccirilli, Benner, et al in their Communication on page 9853 ff.

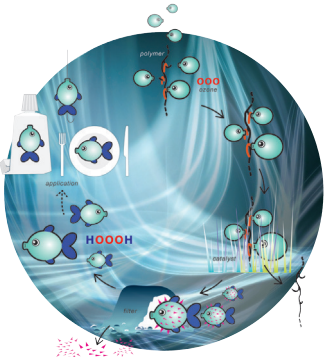

Hydrogen Trioxide

in their Communication on page 9917 ff. G. Strle and J. Cerkovnik describe s simple and efficient preparation of HOOOH on derivatized polystyrene beads

How to contact us:

Editorial Office:
E-mail: angewandte@wiley-vch.de
Fax: (+49) 62 01–606-331
Telephone: (+49) 62 01–606-315

Reprints, E-Prints, Posters, Calendars:
Carmen Leitner
E-mail: chem-reprints@wiley-vch.de
Fax: (+49) 62 01–606-331
Telephone: (+49) 62 01–606-327

Copyright Permission:
Bettina Loycke
E-mail: rights-and-licences@wiley-vch.de
Fax: (+49) 62 01–606-332
Telephone: (+49) 62 01–606-280

Online Open:
Margitta Schmitt
E-mail: angewandte@wiley-vch.de
Fax: (+49) 62 01–606-331
Telephone: (+49) 62 01–606-315

Subscriptions:
www.wileycustomerhelp.com
Fax: (+49) 62 01–606-184
Telephone: 0800 1800536 (Germany only)
+44(0) 1865476721 (all other countries)

Advertising:
Marion Schulz
E-mail: mschulz@wiley-vch.de
Fax: (+49) 62 01–606-550
Telephone: (+49) 62 01–606-565

Courier Services:
Boschstrasse 12, 69469 Weinheim

Regular Mail:
Postfach 101161, 69451 Weinheim

Angewandte Chemie International Edition is a journal of the Gesellschaft Deutscher Chemiker (GDCh), the largest chemistry-related scientific society in continental Europe. Information on the various activities and services of the GDCh, for example, cheaper subscription to *Angewandte Chemie International Edition*, as well as applications for membership can be found at **www.gdch.de** or can be requested from GDCh, Postfach 900440, D-60444 Frankfurt am Main, Germany.

GDCh
Gesellschaft Deutscher Chemiker

Service

Author Profile

"My favorite author (fiction) is Dan Brown. My favorite motto is "Do your best". …"
This and more about Shao Q. Yao can be found on page 9750.

Books

Highlights

Photochromism

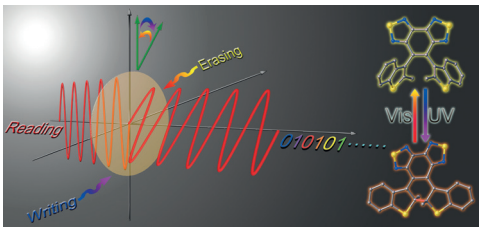

No erasure upon reading: The development of a diaryl benzobis(thiadiazole) derivative with thermally stable isomers that can be isolated owing to intramolecular steric hindrance is summarized in this Highlight. Practically useful photochromic switches that do not suffer from erasure upon reading have thus been fabricated.

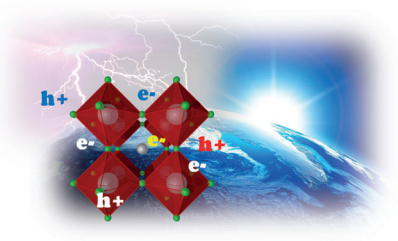

Minireviews

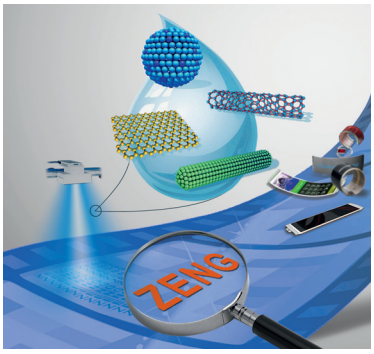

Reviews

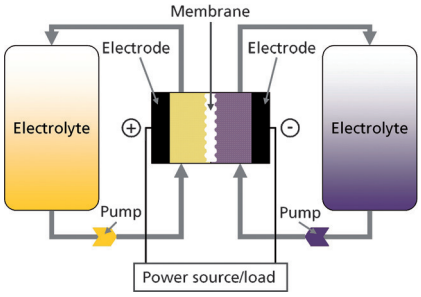

Communications

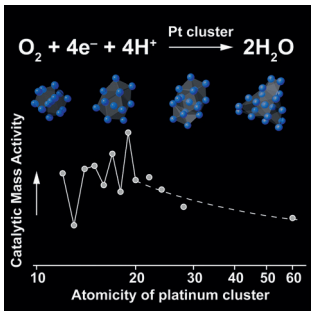

For the USA and Canada:
ANGEWANDTE CHEMIE International Edition (ISSN 1433-7851) is published weekly by Wiley-VCH, PO Box 191161, 69451 Weinheim, Germany. US mailing agent: SPP, PO Box 437, Emigsville, PA 17318. Periodicals postage paid at Emigsville, PA. US POSTMASTER: send address changes to *Angewandte Chemie*, John Wiley & Sons Inc., C/O The Sheridan Press, PO Box 465, Hanover, PA 17331. Annual subscription price for institutions: US$ 11.738/10.206 (valid for print and electronic / print or electronic delivery); for individuals who are personal members of a national chemical society prices are available on request. Postage and handling charges included. All prices are subject to local VAT/sales tax.

Conformational symbiosis: Non-natural heterogeneous backbones obtained by fusing peptidomimetic urea-based helical foldamers to either end of an α-peptide segment fold into a helical structure, spanning the entire sequence in an uninterrupted manner. Only a few urea units are sufficient to propagate a helical conformation along short peptide segments.

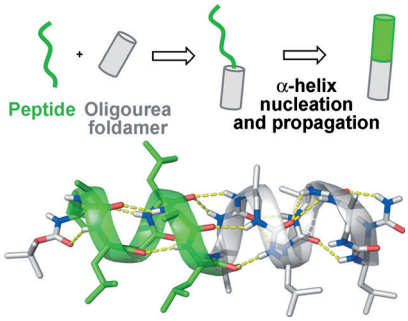

Foldamers

Sugar vibrates: A vibrational probe was developed to visualize glucose uptake activity by stimulated Raman scattering microscopy in living cells and tissues with subcellular resolution. Heterogeneous uptake patterns were observed in neuronal culture and tumor tissues, demonstrating a promising technique to study energy demands in brain and tumors.

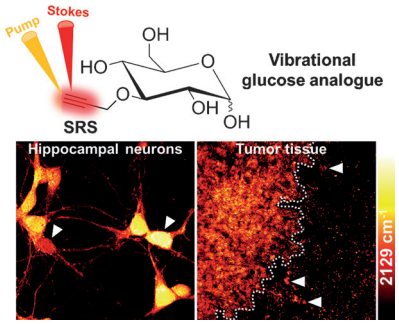

Glucose Uptake

Body of evidence: A body-centered cubic (bcc) gold nanocluster composed of 38 gold atoms protected by 20 adamantanethiolate ligands and two sulfido atoms ($[Au_{38}S_2(SR)_{20}]$, where $R = C_{10}H_{15}$) is revealed by single-crystal X-ray crystallography. This bcc structure is in striking contrast with the fcc structure of bulk gold and conventional Au nanoparticles and gives rises to different electronic properties.

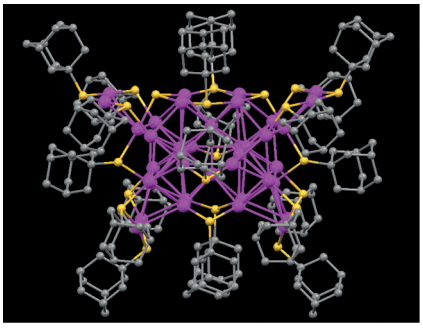

Gold Nanoclusters

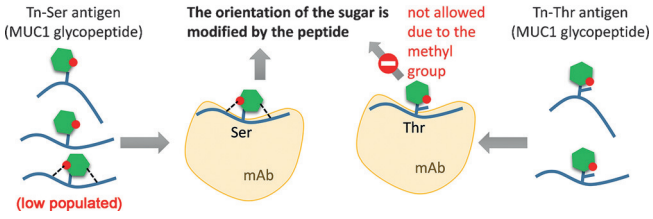

Spot the difference: The structures of two Tn antigen glycopeptides, with *N*-acetylgalactosamine (GalNAc, green hexagon) attached to either Ser or Thr, in complex with an anti-MUC1 antibody are reported. The results reveal significant differences in the conformational behavior of the two glycopeptides in the bound state and demonstrate the non-equivalence of Ser and Thr *O*-glycosylation points in molecular recognition processes.

Glycopeptides

Heterogeneous Catalysis

All about that acid–base: Hf-, Sn-, and Zr-β zeolites promote C–C coupling through reversible metal enolate formation. These materials are shown to catalyze aldol condensations between aromatic aldehydes and acetone with near quantitative yields, even in the presence of water and acetic acid.

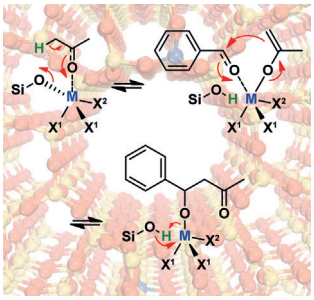

Acylation

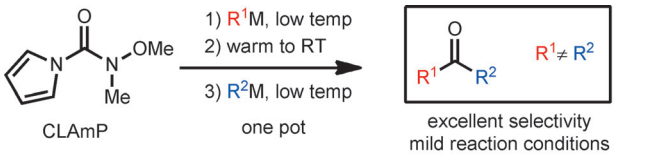

Pot economy: Unsymmetrical ketones are readily and selectively prepared in one pot by the sequential addition of organometallic nucleophiles to *N*-methoxy-*N*-methyl-1*H*-pyrrole-1-carboxamide (CLAmP), a rationally designed carbonyl dication synthetic equivalent which forms tetrahedral intermediates that are persistent at the temperature of nucleophile addition but are kinetically labile at ambient temperature.

Mesoporous Materials

MMONTs (mesoporous metal–organic nanotubes) have been synthesized, starting from $[(phen/bipy)_2Pd_2(NO_3)_2]$ and 4-pyridinyl-3-pyrazole. MMONT structures with outside diameters of up to 4.5 nm and channel sizes of 2.4 nm were constructed by a rational coordination-directed bottom-up fabrication process featuring an unprecedented barrel-to-tube conversion. Pd yellow, N blue, O red.

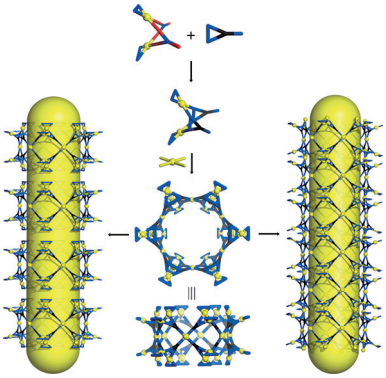

Host–Guest Chemistry

Gate crashers: Activated perethylated pillar[5]arene crystals have been demonstrated to show selective gate-opening behavior depending on alkane shape and length. The activated crystals could quantitatively take up *n*-alkanes with more than five carbon atoms, and *n*-hexane could even be stored under reduced pressure. In contrast, the gate-opening behavior was not observed in the adsorption of cyclic and branched alkanes.

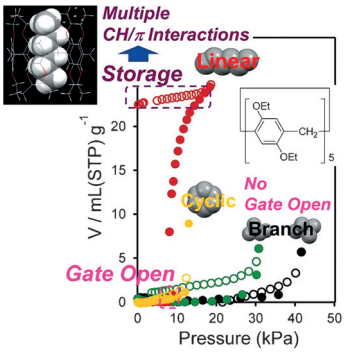

ZiP fasteners: On replacing C:G base with the artificial Z:P pair (blue) a crystal structure (see picture) of the guanosine riboswitch (purple), bound to a hypoxanthine ligand (red), is obtained which can be superimposed on the structure of the native form (green). This is the first crystal structure of an RNA molecule built from a six-nucleotide artificially expanded genetic-information system.

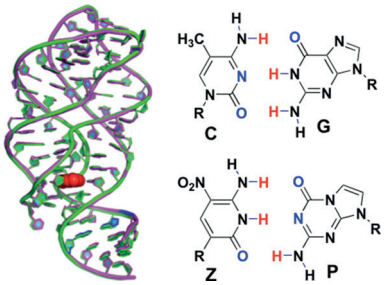

Artificial Base Pairs

Inside Back Cover

Protein design: A novel artificial protein with pseudo-six-fold symmetry creates a nanocrystal of cadmium chloride, sandwiched between two copies of the protein (see picture). X-ray structural evidence for the formation of the nanocrystal inside the protein is presented.

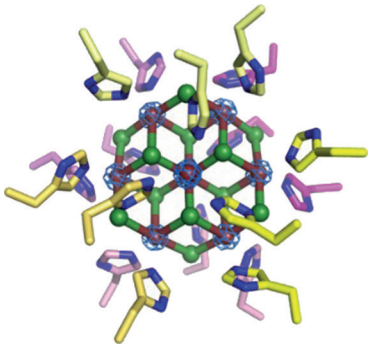

Biomineralization

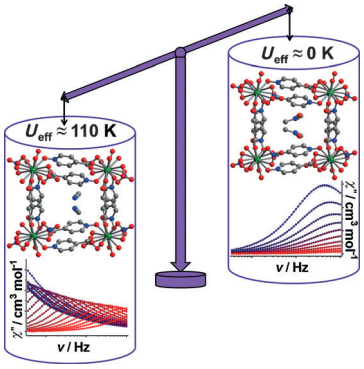

Guest swap: Exchange of the guest molecules within the pores of a metal–organic framework (MOF) featuring Dy_2 single-molecule magnets as nodes imparts major changes in the magnetization relaxation dynamics (see picture; spectra recorded from 2 K (blue plots) to 9 K (red)). As a result of guest exchange, significantly different effective relaxation barriers (U_{eff}) for the compound are measured. Atom colors: Dy = green, O = red, N = blue, C = gray.

Magnetic Properties

A tool-box of reactive base metals: Mo^0, W^0, Fe^0, Ru^0, Re^0, and Zn^0 nanoparticles are prepared with diameters less than or equal to 10 nm. The reaction involves simple metal chlorides and a straightforward liquid-phase synthesis. Subsequent transformation to metal nanoparticle compounds (MoS_2, $FeAs_2$, Re_4Mo) is possible as well.

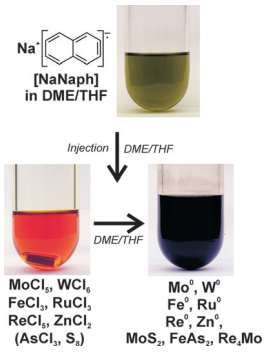

Metal Nanoparticles

Chemical Evolution

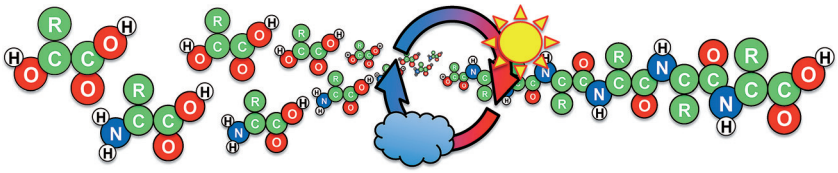

Amino acids form peptide bonds when subjected to day–night cycles (wet–dry cycles) in the presence of hydroxy acids. Such a reaction could have occurred on the prebiotic Earth.

Synthetic Methods

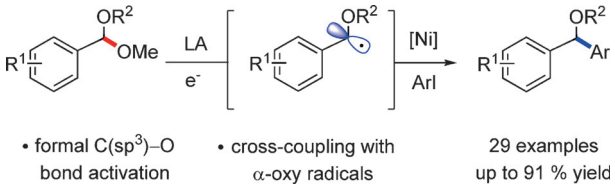

A radical couple: A new substrate class for nickel-catalyzed C(sp^3) cross-coupling reactions is reported. α-Oxy radicals generated from benzylic acetals, TMSCl, and a mild reductant can participate in chemoselective cross-coupling with aryl iodides using a nickel catalyst. The mild reaction conditions and good functional-group tolerance make this an attractive method for dialkyl ether synthesis. LA = Lewis acid, TMS = trimethylsilyl.

Inhibitors

'Diol' EH for virulence: The protein Cif is secreted by *P. aeruginosa* and blocks the endocytic recycling of CFTR, an ion channel required for mucociliary clearance. The ability of Cif to hydrolyze reporter epoxides was shown to be required for virulence, thus indicating a link between epoxides and protein trafficking. A small-molecule inhibitor that protects this key element of airway defenses was identified and could lead to a new therapeutic approach.

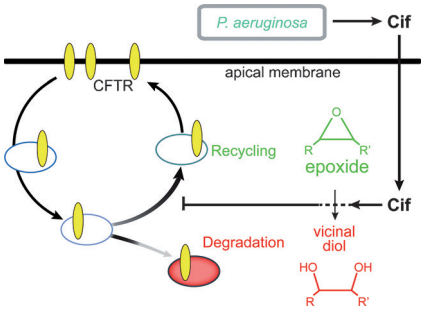

Heterogeneous Catalysis

Teaming up: A combined approach using microfocus X-ray fluorescence and X-ray diffraction computed tomography has been employed to image an industrial hydrogenation catalyst (Mo-promoted Pt/C) under liquid-phase operating conditions for the first time. The nature and distribution of the active state of the catalyst and promoter have been spatially resolved at the micrometer scale (see picture).

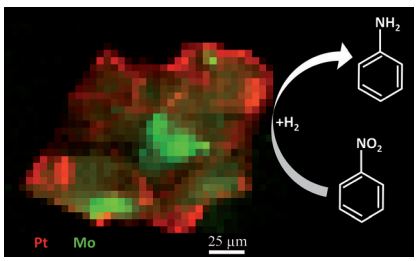

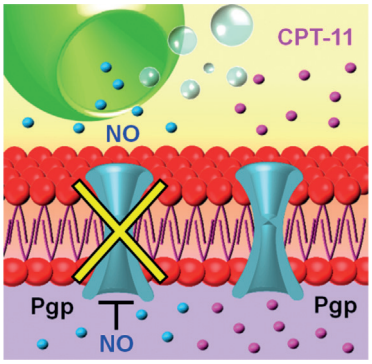

Two is better than one: A carrier system is developed that can generate NO bubbles in the acidic environment of tumor tissues to trigger localized drug release (specifically irinotecan, denoted CPT-11) and to reverse Pgp-mediated multidrug resistance (Pgp = P-glycoprotein). The combined system enhances intracellular drug accumulation in cancer cells so that the concentration exceeds the therapeutic threshold, eventually leading to antitumor activity.

Drug Delivery

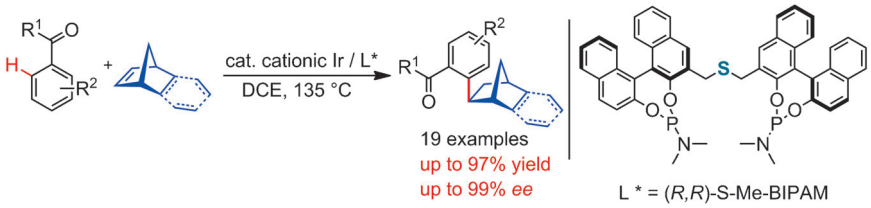

Linked up: Asymmetric intermolecular hydroarylation of bicycloalkenes by C–H bond cleavage has been developed. The use of a chiral sulfur-linked bis(phosphoramidite) ligand (L*) led to excellent enantioselectivity. Notably, the hydroarylation of 2-norbornene with *N*,*N*-dialkylbenzamide proceeds with high selectivity for the mono-*ortho*-alkylation product. DCE = 1,2-dichloroethane.

Asymmetric C–H Functionalization

Pass the sugar: The crystal structure of a native ternary complex of a glycosyltransferase, the retaining glucosyl-3-phosphoglycerate synthase GpgS, in a productive mode for catalysis was obtained. By combining structural, chemical, and enzymatic methods, as well as molecular dynamics and QM/MM calculations, the catalytic mechanism was unraveled and the results provide strong experimental support for a front–side substrate-assisted S_Ni-type reaction.

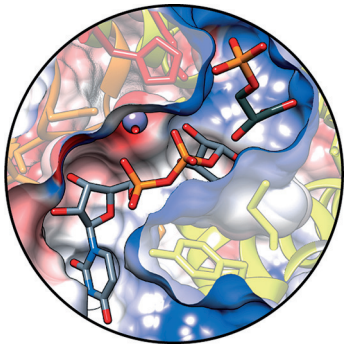

Enzyme Catalysis

Guiding light: A biocompatible carbon nanotube (CNT)-liposome supramolecular nanohybrid that penetrates into cells was developed. The nanohybrid can be loaded with functional molecules and controlled by laser light. Photo-induced release of amiloride (red stars) from the nanohybrid led to the inactivation of amiloride-sensitive neurons in *C. elegans*. This prototype could inspire the development of biologically active nanorobots for the manipulation of organisms.

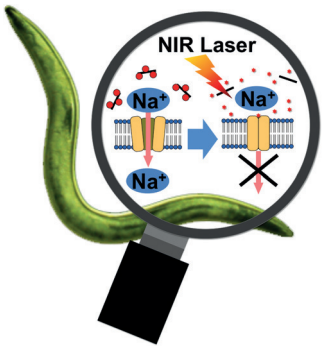

Nanotechnology

Oxygen Reduction

A non-precious Fe/N/C electrocatalyst was prepared through pyrolysis of $Fe(SCN)_3$, poly-*m*-phenylenediamine, and carbon black. The obtained Fe/N/C catalyst has high level of S doping and high surface area, and thus exhibits excellent catalytic activity for the oxygen reduction reaction in acidic solution. A polymer electrolyte membrane fuel cell using this catalyst as the cathode can yield a maximal power density as high as 1.03 $W cm^{-2}$.

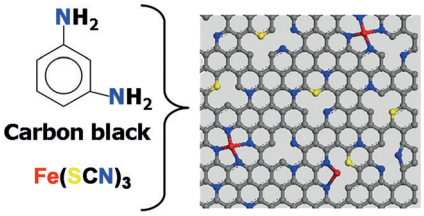

Na-Ion Battery

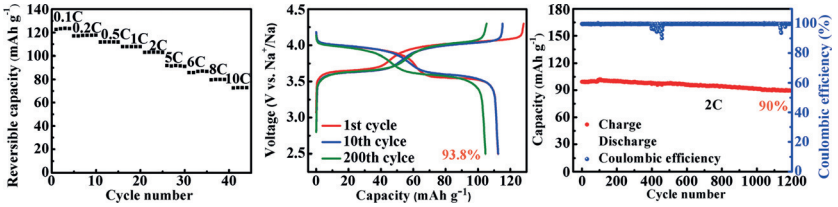

A solvothermal low-temperature strategy was used for the synthesis of a series of $Na_3(VO_{1-x}PO_4)_2F_{1+2x}$ $(0 \le x \le 1)$ nanoparticles. The as-synthesized $Na_3(VOPO_4)_2F$ shows the best Na-storage performance in terms of both high rate capability (up to 10C rate) and long cycle stability over 1200 cycles reported so far.

Hydrogen Trioxide

Back Cover

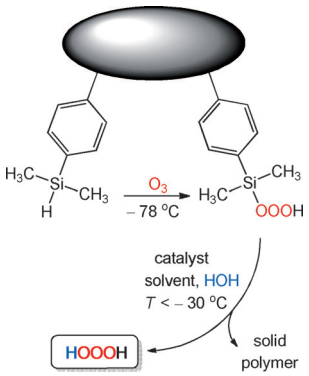

O_3 can do: Hydrogen trioxide (HOOOH) is prepared on functionalized polymer beads and subsequently released. Solutions of high-purity HOOOH in diethyl ether, free of any reactants and by-products, may be stored at −20 °C for weeks. HOOOH could be also isolated in highly pure form or dissolved in another solvent, thus significantly extending the research perspectives of HOOOH.

Single-Molecule Studies

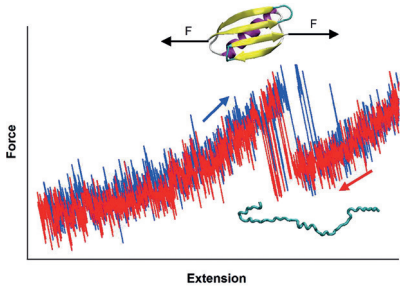

Pushmi-pullyu protein: Using low drift cantilevers, the two-state unfolding and refolding of a small α/β protein NuG2 is directly observed in single-molecule atomic force microscopy experiments.

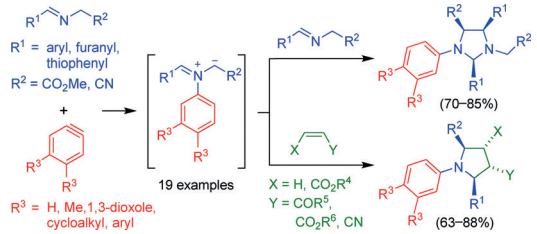

Two steps in one flask: A sequence of arylation of a Schiff base, an intramolecular proton transfer from the methylene position to the anionic aryne ring, and reaction of the resulting ylide with either a second equivalent of Schiff base or an electron-deficient alkene in a (3+2) cycloaddition generates imidazolidines and pyrrolidines in high stereoselectivity and 63–88% yields.

1,3-Dipolar Cycloaddition

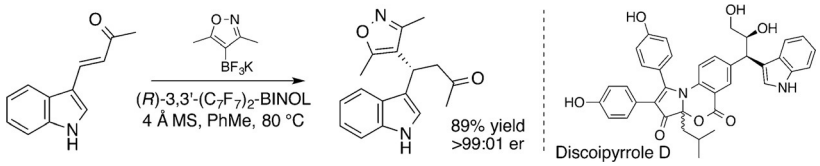

Fluoride has to go: Bis-heteroaryl or bis-aryl stereocenters are formed through an organocatalytic enantioselective conjugate addition using heteroaryl or aryl trifluoroborate salts, respectively, as nucleophiles. Control experiments suggest that fluoride dissociation in the anhydrous conditions is necessary. The reaction was applied toward the synthesis of discoipyrrole D, an inhibitor of DDR2-dependent migration of BR5 fibroblasts.

Enantioselective Synthesis

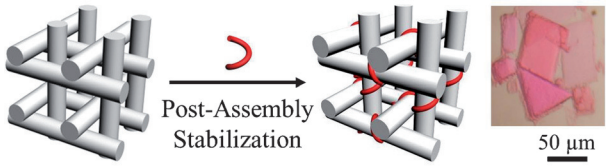

Added stability: Owing to weak inter-unit cohesion, self-assembled DNA crystals tend to be fragile. Such nanostructures can be effectively stabilized by the addition of a molecule that binds to the cohesive sites and stabilizes the inter-unit interactions. Whereas the original DNA crystals are only stable in solutions of high ionic strength (e.g., ≥ 1.2 M $(NH_4)_2SO_4$), the stabilized crystals are stable at much lower ionic strengths.

DNA Structures

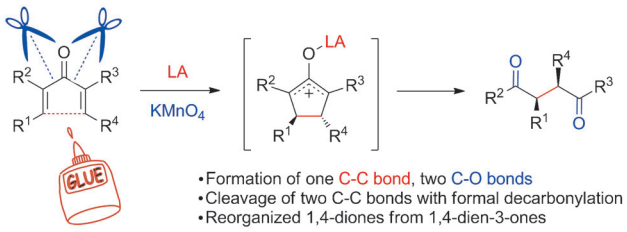

Cut and paste with manganese and iron: A new example of interrupted Nazarov reaction is described, involving oxidative cleavage of the oxidocyclopentenyl intermediate to produce 1,4-diketones. Simple treatment of cross-conjugated dienones with $FeCl_3 \cdot 6H_2O$ and $KMnO_4$ at low temperature affords the products under convenient conditions.

Nazarov Reaction

Heterocycles

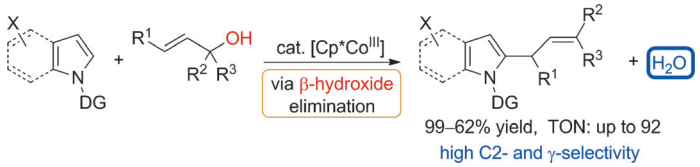

The unique reactivity of [Cp*Co^{III}] versus [Cp*Rh^{III}] is showcased in the direct dehydrative C–H allylation with non-activated allyl alcohols. Cationic [Cp*Co^{III}] gave C2-allylated indoles, pyrrole, and phenyl-pyrazole in good yields, while the analogous [Cp*Rh^{III}] catalysts were not effective. The high γ-selectivity and C2-selectivity result from directing-group-assisted C–H metalation, insertion of a C–C double bond, and subsequent β-hydroxide elimination. Cp* = C_5Me_5.

Polymerization

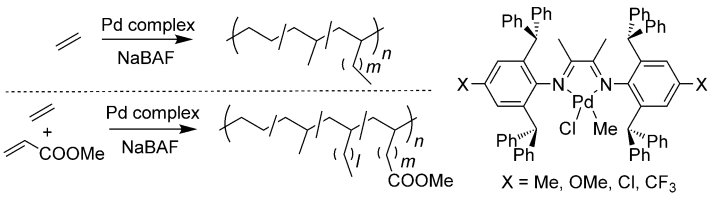

Slow and steady wins the race: A series of palladium complexes with bulky α-diimine ligands promoted the title reactions (see scheme; NaBAF = sodium tetrakis(3,5-bis(trifluoromethyl)phenyl)borate). The catalysts showed extremely high activity and thermal stability, and the resulting polymers had a high molecular weight, very low branching density, and unique microstructures.

Synthetic Methods

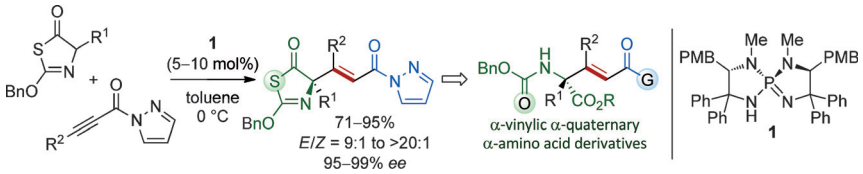

A broadly applicable, highly *E*-selective and enantioselective conjugate addition of 2-benzyloxythiazol-5(4*H*)-ones to β-substituted alkynyl *N*-acyl pyrazoles was developed. A *P*-spiro chiral iminophosphorane **1** is used as the catalyst. This method leads to structurally diverse, optically active α-amino acid derivatives bearing a geometrically defined trisubstituted olefinic component at the α-position. PMB = *p*-methoxybenzyl.

1,4-Rhodium(III) Migration

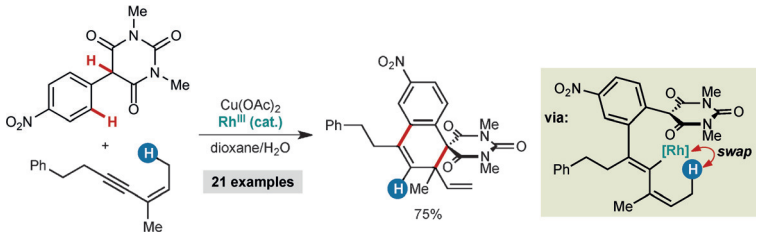

All for one and 1,4-all(yl): 1,3-Enynes containing allylic hydrogens *cis* to the alkyne act as three-carbon components in rhodium(III)-catalyzed, all-carbon [3+3] oxidative annulations to produce spirodialins. The proposed mechanism of these reactions involves the alkenyl-to-allyl 1,4-rhodium(III) migration.

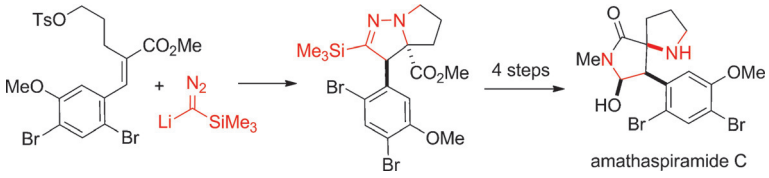

Three bonds, one step: Bicyclic pyrazolines, as a latent form of the α-*tert*-alkylamino acid moiety of the amathaspiramides, are efficiently constructed from an α,β-unsaturated ester and lithium(trimethylsilyl)diazomethane through a formal [3+2] cycloaddition. Protonolytic N–N bond cleavage followed by imide formation from nitrile hydrolysis, N-methylation, and reduction of one of the imide carbonyl groups leads to a total synthesis of amathaspiramide C.

Natural Product Synthesis

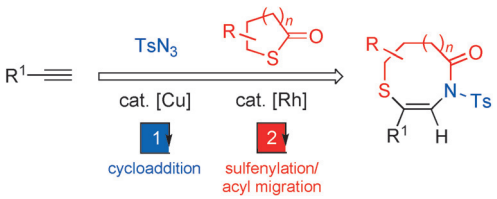

Expansion project: *N*-Sulfonyl-1,2,3-triazoles react with thioesters in the presence of a rhodium(II) catalyst to produce β-sulfanyl enamides in a stereoselective manner. The method is successfully applied to a ring-expansion reaction of thiolactones (see Scheme; Ts = 4-toluenesulfonyl), thus leading to the formation of sulfur-containing lactams.

Synthetic Methods

In depth: Dragmacidin D is a marine bis(indole) alkaloid originating from species of the deep-sea sponge genus *Dragmacidon*. The stereochemical identity and properties of dragmacidin D have remained elusive since its isolation. The 10-step enantioselective total synthesis of (+)-dragmacidin D by direct asymmetric enediolate alkylation affords additional data on the stereochemistry of this marine alkaloid.

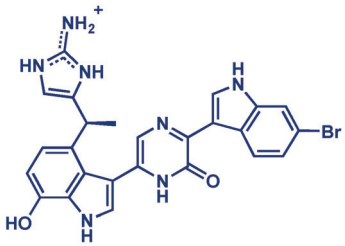

(*S*)-dragmacidin D

Asymmetric Synthesis

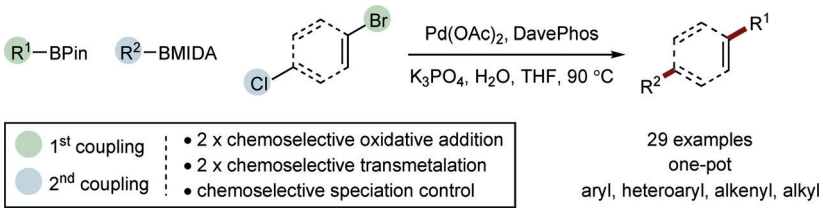

Breaking the limit: Chemoselective Suzuki–Miyaura cross-coupling has previously been limited to single C–C bond formation due to a lack of nucleophile selectivity. Manipulation of boron speciation enables complete chemoselective control of the Suzuki–Miyaura reaction, allowing harmonized sequential cross-coupling in a single operation.

Sequential Cross-Coupling

Silicon Compounds

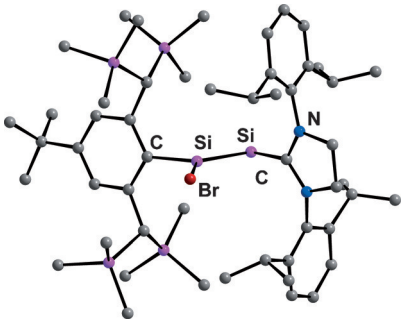

Double reduction: The NHC-stabilized disilavinylidene (*Z*)-(SIdipp)Si=Si(Br)Tbb (SIdipp = C[N(C_6H_3-2,6-*i*Pr_2)CH_2]$_2$; Tbb = C_6H_2-2,6-[$CH(SiMe_3)_2$]$_2$-4-*t*Bu; NHC = N-heterocyclic carbene) has been synthesized and characterized. The compound was prepared by two-electron reduction of the NHC-stabilized bromo(silyl)silylene $SiBr(SiBr_2Tbb)(SIdipp)$. $SiBr(SiBr_2Tbb)$-(SIdipp) was obtained upon treatment of $SiBr_2$(SIdipp) with (*E*)-Tbb(Br)Si=Si(Br)Tbb or LiTbb.

Aromatic Rhodacycles

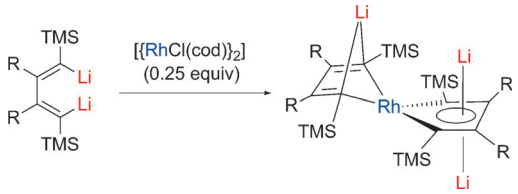

Give and take: Dilithio reagents that are a type of 1,3-butadienyl dianion react with [{RhCl(cod)}$_2$] to give aromatic dilithio rhodacycles. In this process, the dilithio compounds behave as non-innocent ligands and formal oxidants. Thus organolithium compounds with suitable π conjugation can act as electron acceptors.

Halex ^{18}F-Fluorination

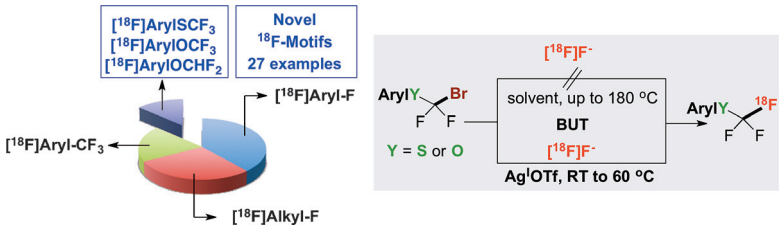

A halogen exchange (halex) ^{18}F-fluorination process offers access for the first time to ^{18}F-labeled arylOCF$_3$, arylOCHF$_2$ and arylSCF$_3$, three motifs of established medicinal importance in PET radiotracers. The use of silver(I) triflate is critical to permit ^{18}F-labeling under mild conditions.

Acyclic Stereoselection

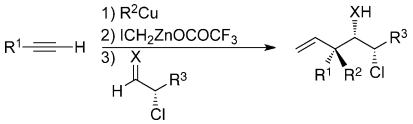

All-carbon quaternary stereocenter: The combined carbometalation/zinc homologation of alkynes followed by reactions with α-heterosubstituted aldehydes and imines provides access to functionalized acyclic adducts. These adducts obtained in a single-pot reaction have three new carbon–carbon bonds and two to three stereogenic centers, including a quaternary carbon stereocenter.

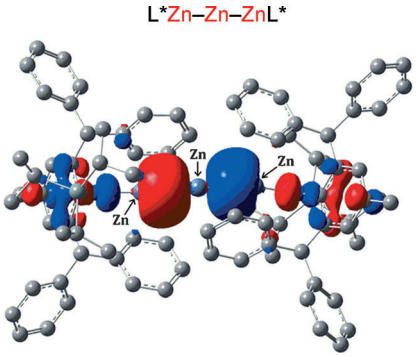

Form an orderly queue! Reduction of an extremely bulky amido (L*) zinc bromide complex, [L*ZnBr] with a magnesium(I) dimer yields the formally zinc(0) complex, [L*ZnMg(MesNacnac)], which contains the first example of an unsupported Zn–Mg bond. Its subsequent reaction with $ZnBr_2$ affords the unprecedented mixed-valence, linear tri-zinc complex, [L*Zn^{I}Zn^{0}Zn^{I}L*] (see picture).

Metal–Metal Bonds

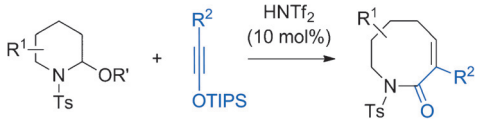

Growth rings: A mild catalytic synthesis of medium-ring lactams through ring expansion of cyclic hemiaminals was developed. This synthetically useful method also gives insight into the reactivity of both siloxy alkynes and *N*-acyliminium analogues.

Synthetic Methods

I should COCO: Reaction between a β-diketiminato magnesium hydride and carbon monoxide results in the isolation of a dimeric *cis*-enediolate species through the reductive coupling of two CO molecules. Under catalytic conditions with $PhSiH_3$, an observable magnesium formyl species may be intercepted for the mild reductive cleavage of the CO triple bond.

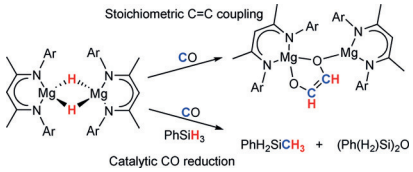

Homogeneous Catalysis

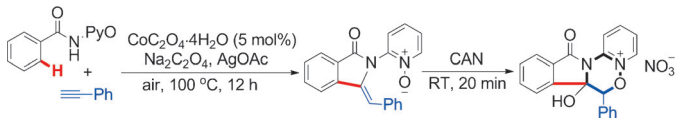

Directing group and Co: The title reaction proceeds in the presence of an N,O-bidentate directing group. This method is characterized by wide substrate scope and cheap cobalt catalysts, and offers a new approach to 3-methyleneisoindolin-1-one, which can be converted into an oxadiazine salt in one step. Moreover, the directing group can be removed in three steps. CAN = ceric ammonium nitrate.

C–H Activation

Unusually Protective: In the search for a glycan epitope for protection against *Streptococcus pneumoniae* serotype 4, total synthesis of the repeating unit (see structure) enabled the identification of pyruvate as a crucial determinant of immunogenicity. This lays the foundation for the development of a new antibacterial vaccine candidate against *Streptococcus pneumoniae* serotype 4.

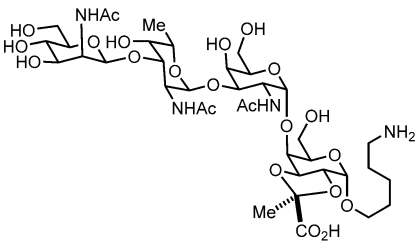

Carbohydrate Immunology

Structure Elucidation

Treasure quest: The complementary use of electron diffraction and microfocused synchrotron radiation enables innovative and accurate structure analyses of novel compounds in heterogeneous microcrystalline materials. The sulfide telluride $Pb_8Sb_8S_{15}Te_5$ was discovered this way. It adopts an unusual tetragonal structure type with building blocks that resemble NaCl-type fragments as well as chain-like units typical for sulfides.

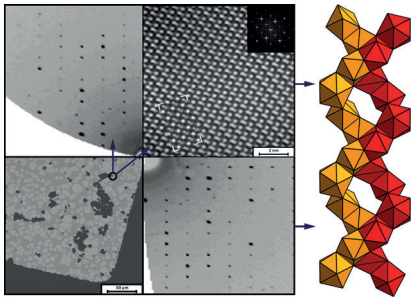

MicroRNA Detection

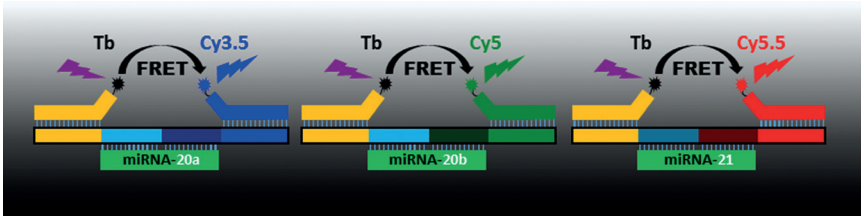

A suitable timeframe: An amplification-free homogeneous "mix-and-measure" assay for the multiplexed detection of up to three microRNAs has been developed. It uses Förster resonance energy transfer from a Tb complex donor to three different dye acceptors and is conducted in one step and at a single temperature.

Synthetic Biology

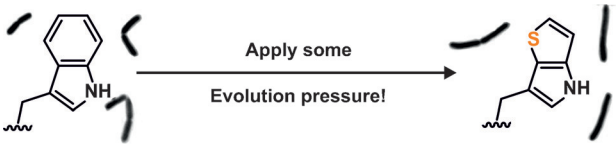

Towards synthetic bacteria: An evolution experiment in synthetic medium led to quantitative substitution of tryptophan with L-β-(thieno[3,2-*b*]pyrrolyl)alanine in response to 20899 TGG codons in bacterium *Escherichia coli W3110*. The evolved bacteria showed robust growth in the complete absence of Trp without significant adverse effects on the cellular survival.

Supporting information is available on www.angewandte.org (see article for access details).

This article is accompanied by a cover picture (front or back cover, and inside or outside).

A video clip is available as Supporting Information on www.angewandte.org (see article for access details).

The Very Important Papers, marked VIP, have been rated unanimously as very important by the referees.

This article is available online free of charge (Open Access).

The Hot Papers are articles that the Editors have chosen on the basis of the referee reports to be of particular importance for an intensely studied area of research.

Angewandte Corrigendum

Upon review of a publication from the Pattenden group[1] and upon further examination of 2D NMR data for the compounds reported in this Communication, the authors are prompted to make three structural reassignments:
Compound **18**, shown as 18-acetoxycoralloidolide A, should be 19-acetoxycoralloidolide A. Compound **19**, shown as 18-hydroxycoralloidolide A should be 19-hydroxycoralloidolide A. Compound **20**, shown as 18-oxobipinnatin J should be 19-oxobipinnatin J. The authors are sorry for the misassignment of these by-products. The total synthesis of coralloidolides A, B, C, and E stands as reported.

[1] Y. Li, G. Pattenden, J. Rogers, *Tetrahedron Lett.*, **2010**, *51*, 1280.

Total Synthesis of Coralloidolides A, B, C, and E

T. J. Kimbrough, P. A. Roethle, P. Mayer, D. Trauner* ——— **2619–2621**

Angew. Chem. Int. Ed. **2010**, *49*

DOI: 10.1002/anie.200906126

Angewandte Corrigendum

In Figure 1 of this Communication, the values at the vertical axis must be multiplied by 10; the corrected version of Figure 1 is shown below. Accordingly, the description in text for Figure 1 (page 1618, left column, 2nd paragraph) should also be corrected as follows:
"We also examined the CD spectra of these compounds and found that (*R*)-**3 aa** showed a relatively weak negative Cotton effect at $\lambda = 259$ nm ($\Delta\varepsilon = -30\ M^{-1}cm^{-1}$), whereas (*R*,*R*)-**9** showed stronger positive and negative Cotton effects at $\lambda = 282$ nm ($\Delta\varepsilon = +73\ M^{-1}cm^{-1}$) and $\lambda = 256$ nm ($\Delta\varepsilon = -108\ M^{-1}cm^{-1}$), respectively (Figure 1)."
This correction does not change any conclusion of this Communication.

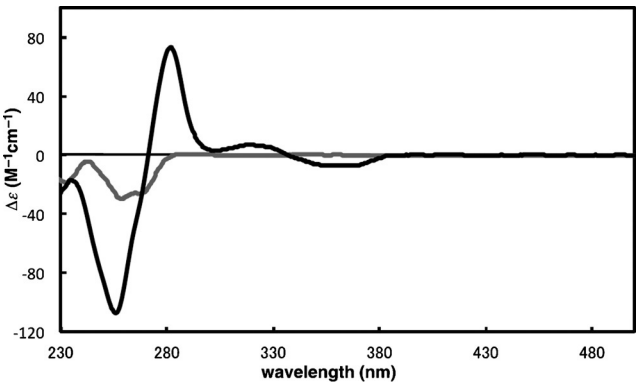

Figure 1. CD spectra of (*R*)-**3 aa** (gray line; 1.1×10^{-5} M) and (*R*,*R*)-**9** (black line; 5.7×10^{-6} M) in CH_2Cl_2 at 25 °C.

Rhodium-Catalyzed Asymmetric Synthesis of Silicon-Stereogenic Dibenzosiloles by Enantioselective [2+2+2] Cycloaddition

R. Shintani,* C. Takagi, T. Ito, M. Naito, K. Nozaki* ——— **1616–1620**

Angew. Chem. Int. Ed. **2015**, *54*

DOI: 10.1002/anie.201409733

